

# The potential mechanism of PPP2R3A in myocardial cells and its interacting proteins

C.-Y. WU<sup>1,2,3</sup>, Y. LIANG<sup>1</sup>, X.-F. LI<sup>1</sup>, G.-B. SONG<sup>1,2,3</sup>

<sup>1</sup>Department of Clinical Laboratory, First Affiliated Hospital of Kunming Medical University, Kunming, China

<sup>2</sup>Yunnan Key Laboratory of Laboratory Medicine, Kunming, China

<sup>3</sup>Yunnan Innovation Team of Clinical Laboratory and Diagnosis, First Affiliated Hospital of Kunming Medical University

**Abstract.** – **OBJECTIVE:** PPP2R3A plays a key role in the cardiac pathological and physiological processes, yet little is known about how the protein involved in normal myocardium formation and the protein-protein interaction pathways involved. To address this issue, we investigated the role of PPP2R3A in cardiac myocytes and identify PPP2R3A specific protein interaction partners to accelerate the developmental process of the mechanistic studies.

**MATERIALS AND METHODS:** PPP2R3A-silenced primary myocardial cell of neonatal rats and H9c2 cells were established by infecting shRNA lentiviral particles. RT-PCR and Western blot were used to determine the expression of PPP2R3A and silencing efficiency. The cell viability was analyzed by CCK-8 kit, then the cell cycles and apoptosis assays were detected by flow cytometry. Novel protein-protein interactions of PPP2R3A were detected by Yeast Two-Hybrid assays using a high-quality human primary cardiomyocyte cDNA library.

**RESULTS:** PPP2R3A-silencing rat primary cardiomyocytes and H9c2 cells were established successfully, and the expression of PPP2R3A was downregulated significantly as confirmed by RT-PCR and Western blot. PPP2R3A silencing can inhibit the myocardial cell proliferation, arrest the cell cycle in the S phase and promote the cardiomyocytes apoptosis. 19 potential candidates like COL1A2, GIPC1 and BCL6 specifically interact with PPP2R3A, and COL1A2 was the highest screening frequency, covering 12.5% of the 24 clones. These partners are highly enriched in signaling pathways associated with a variety of cellular processes.

**CONCLUSIONS:** A series of studies have discovered that PPP2R3A was closely associated with heart failure and arrhythmia. Our data further confirmed PPP2R3A plays an important role in the cardiomyocytes and PPP2R3A in the regulation of cardiac events via its interaction partners. Therefore, it is a potential therapeutic target for the disease.

*Key Words:*

PPP2R3A, Cardiomyocytes, Myocardial function, Biomarker, Yeast two-hybrid assay.

## Introduction

Protein phosphatase 2A (PP2A), one of the major serine/threonine phosphatases in mammalian cells, are responsible for the majority of dephosphorylation events in the human heart. The structure of PP2A is composed of three subunits: catalytic (C), scaffold (A), and a variable regulatory B subunit from four distinct families that controlled substrate specificity, influenced enzyme activity, and subcellular localization<sup>1</sup>. PP2A plays an important role in cardiac physiology. It can regulate cardiac excitability through dephosphorylation of cardiac ion channels, transporters, and their respective regulatory proteins<sup>2</sup>; its activity is also requisite for cardiac contractility and relaxation<sup>3</sup>.

Both *in vivo* and *in vitro* studies have illustrated that PP2A regulatory subunit activity is critical for mature PP2A holoenzyme function. Loss of the regulatory subunits has been linked to cardiac pathological changes. When lacked the B56γ regulatory subunit of PP2A, the mice had a defect in the formation of the ventricular septum of the heart and a decrease in the number of ventricular cardiomyocytes<sup>4</sup>. Excessive B56α in mice decreases PP2A activity, resulting in increased heart rate, and decreased parasympathetic activity<sup>3</sup>. In addition, the elevated expression levels of PP2A subunits were observed in heart failure, including PPP2R5A, PPP2R5B, PPP2R5E, PPP2R3A, and PPP2R4<sup>2</sup>.

Protein phosphatase 2 regulatory subunit B''alpha (PPP2R3A), which belong to the B''-family of PP2A regulatory subunits, harbored two major specific splice products – PR72 (B''α2) and large transcript PR130 (B''α1)<sup>5</sup>. They share an identical C terminus and are highly expressed in human heart. In the heart, PR130 was reported to mediate dephosphorylation of type 2 ryanodine receptor (RyR2), which was centrally involved in the myocyte exci-

tation-contraction coupling process, suggesting that PR130 may play crucial roles in cardiac contractile function<sup>6</sup>. A new study<sup>7</sup> showed that PR130-knock-out zebrafish exhibited cardiac looping defects and decreased cardiac function (decreased fractional area and fractional shortening). Taken together, these studies raised the possibility that PPP2R3A might be an important regulator of cardiac development and functions, but it remains unclear how it impacts on cardiac physiology. Here, we used a shRNA specific sequence targeting PPP2R3A to explore its key role in cardiac function *in vitro*. Subsequently, we identified PPP2R3A potential interacting proteins to characterize its functions. Together, our results provide evidence that the control of heart physiology by PPP2R3A may be the potential novel drug target for heart disease.

## Materials and Methods

### **Ethical Considerations**

All neonatal SD rats (within 7 days) were obtained from animal experiment center of Third Military Medical University. The experiment was carried out under the guidelines of the Ethical and Animal Welfare Committee of the Kunming Medical University.

### **Isolation and Culture of Primary Myocardial Cell of Neonatal Rats**

Fresh cardiac apex of neonatal rats was washed and minced into small pieces in a sterile 90-mm plastic dish. Phosphate-buffered saline (PBS) (1X) containing 10% penicillin and streptomycin were added and were followed by repeatedly digested with 0.125% EDTA-trypsin (digest for 5 minutes at a time and a total of 8 to 10 times). The disaggregated tissue suspension was centrifuged at 1000 rpm for 5 min and the pelleted cells were resuspended in DMEM medium containing 10% fetal bovine serum (FBS) and 100 U/ml penicillin-streptomycin solution. These cell suspensions were seeded in 25 cm<sup>2</sup> culture flasks and incubated at 37°C in humidified atmosphere of 5% CO<sub>2</sub> and 95% air for 90 minutes. The formed adherent cell monolayer was cardiac fibroblasts and cardiac myocytes existed in the supernatant. The supernatant was placed in 25 cm<sup>2</sup> culture flasks and cultures were maintained in a humidified atmosphere of 5% CO<sub>2</sub> at 37°C. Cell culture was observed daily by a phase-contrast microscopy. The medium was changed every 3 days depending on the cell growth rate.

### **Identification of Primary Cardiomyocyte**

The slides of cells that had prepared were washed with PBS (1X) for 3 times and fixed with 4% paraformaldehyde at room temperature for 15 minutes, followed by rinsed gently in PBS. The cells were permeabilized with 0.5% triton X-100 in PBS for 15 min and blocked in 6% normal goat serum in PBS for 30 min at room temperature. The Anti  $\alpha$ -actin antibody was diluted with immunofluorescence primary antibody diluent (1:100) and was added to the cells 4°C for the night. After washing the cells with PBS (1X), they were stained with fluorescent labeled secondary antibody Anti Alexa Fluor 647 (diluted by 1:800 with immunofluorescence second antibody diluent) and incubated at room temperature for 30 minutes. The cells have to be washed for 3 min with PBS and stained with 4',6-diamidino-2-phenylindole (DAPI) (1  $\mu$ g/ml) for 5 minutes in the dark. The antifade mounting medium were applied to mount cover glasses, then, it was observed by confocal microscopy.

### **Culture of Cardiomyocyte-like H9c2 Cells**

The H9c2 cell line were obtained from Cell Bank of Chinese Academy of Sciences (Shanghai, China). Cells were cultured in DMEM medium supplemented with 10% Fetal Bovine Serum (FBS) and 100 U/ml penicillin-streptomycin solution in 25 cm<sup>2</sup> culture flasks at 37°C in a humidified atmosphere of 5% CO<sub>2</sub>. The medium was changed every 2-3 days, and cells were subcultured when they reached 80% confluence.

### **Transfection of shRNA Vector**

The siRNA sequences used to knock down *ppp2r3a* were 5'-CATAATTGCCAAGGTAATCA-3' (*ppp2r3a*-si1#), 5'-GAAGGTTTCACAGCATAATT -3' (*ppp2r3a*-si2#), 5'-CTGTGTTTCTAACTGGAATA-3' (*ppp2r3a*-si3#). The sequence of the control siRNA targeting sequence was 5'-TTCTCCGAACGTGTCACGT-3'. These siRNA sequences were cloned into the pGLV3 vector with green fluorescent protein (GFP), then, they were co-transfected with PG-p1-VSVG, PG-P2-REV, PG-P3-RRE vectors into 293T cells, to obtain lentivirus particles. The identity of the resulting pGLV3-*ppp2r3a*-RNAi construct was verified by sequencing. They were applied to transfect rat primary cardiomyocytes and H9c2 cells, and successfully established *ppp2r3a* downregulated cell lines. All these constructs were purchased from Western Biomedical technology (Chongqing, China).

### **Quantitative Real-Time PCR**

Total RNA from cultured cells was extracted using the TRIzol reagent (Beyotime, China) according to the manufacturer's instructions and quantified by NanoDrop (Thermo Scientific, USA). cDNAs were generated using a PrimeScript RT reagent kit (Takara, Japan). Sequences were as follows: *ppp2r3a* forward 5'-GACATCTTTGCGAAGGGACC-3', reverse 5'-GACTTCAGCCTCTTCTTAAACCG-3';  $\beta$ -actin forward 5'-CCCATCTATGAGGGTTACGC-3', reverse 5'-TTTAATGTCACGCACGATTTC-3'. Quantified analysis was performed in triplicate on the ABI 7300 Fast Real-time PCR system (ABI, USA). The comparative CT method was quantified *ppp2r3a* expression and normalized the CT value to the housekeeping gene  $\beta$ -actin.

### **Western Blotting Analysis**

Cells (untreated/treated rat primary cardiomyocytes and H9c2) were homogenized on ice in the RIPA buffer (Beyotime, Shanghai, China). Insoluble material was removed by centrifugation at 4°C for 15 minutes. The protein concentration was measured using a BCA protein assay (Beyotime, China). Protein was separated on 8% acrylamide gel and transferred to 0.45  $\mu$ m PVDF membranes, and the membranes were blocked for 2h at room temperature with 5% nonfat dry milk in Tris Buffered Saline with Tween (TBST). Membranes were incubated with diluted primary antibodies (rabbit anti-ppp2r3a: 1:500) (Abcam, Cambridge, MA, USA) overnight at 4°C. The secondary antibodies (anti-rabbit IgG: 1:1000) (Sigma-Aldrich, St. Louis, MO, USA) was added and incubated for 1.5 h at room temperature and proteins were visualized by ECL Western Blotting Substrate. Rabbit anti- $\beta$  Actin (1:1000 dilution) (Abcam, Cambridge, MA, USA) was used to normalize the amount of sample loaded.

### **Cell Proliferation Assay**

The cells, including untreated and treated rat primary cardiomyocytes and H9c2 cells, were plated into 96-well plates at  $1.0 \times 10^4$  cells/well (90  $\mu$ l/well) and cultured at 37°C in a humidified atmosphere of 5% CO<sub>2</sub> for 24h. Next, the culture medium was replaced with of fresh medium, and 10  $\mu$ l CCK-8 solution (Sigma-Aldrich, St. Louis, MO, USA) was added to the culture medium and incubated for another 2 h at 37°C. The absorbance was measured using a Multiscan Spectrum (Thermo Fisher Scientific, Waltham, MA, USA) at a wave-length of 450 nm.

### **Cell Cycle Assays**

Cultured cells were harvested and resuspended in PBS solution. Cell suspension at a density of  $3 \times 10^5$ /ml were fixed with 70% precooled ethanol (0-4°C) for more than 2h, stained with PI (BD Biosciences, Franklin Lakes, NJ, USA) and incubated in the dark for 30 minutes. Samples were analyzed on flow cytometer (FCM) with ModFit V3.0 Software to separate G0/G1, S, and G2/M phases.

### **Cell Apoptosis Assays**

Annexin V-PE/7-amino-actinomycin D(7-AAD) staining was performed according to the manufacturer's instructions (BD, Franklin Lakes, NJ, USA). Cell suspension at a density of  $3 \times 10^5$ /ml were stained with 50  $\mu$ l of binding Buffer as well as 5  $\mu$ l 7-AAD and incubated in the dark. After 15 minutes, 450  $\mu$ l binding buffer were added to cell suspension, and mixed with 1  $\mu$ l Annexin V-PE for 15 min in the dark. The flow cytometer was employed to determine the apoptosis ratio.

### **Human Primary Cardiomyocytes cDNA Library Construction**

The libraries were prepared using total RNA extracted from human primary cardiomyocytes. The purified mRNA as a template was used for double strand (ds) cDNA synthesis. Purified ds cDNA and pGADT7-Rec (Clontech, San Jose, CA, USA) were co-transformed into prey yeast cells. Monoclonal colonies were selected for PCR amplification. The inserted sequences in the plasmids were amplified by PCR using specific primers (F: TAATACGACTCACTATAGGGCGAGCG; R: GTGAACTTGCG GGGTTTTTCAGTAT).

### **Yeast Two-Hybrid Assays and Identification of Positive Interactors**

Human PPP2R3A cDNA was amplified by PCR; the PCR fragment was then digested with Sfi I and inserted into the pGBKT7 vector (Clontech, San Jose, CA, USA) to generate a construct of human PPP2R3A cDNA fused frame to the Gal4 DNA-binding domain as the bait. The yeast AH109 strain was transformed with the bait plasmid and mated with the prey plasmid pGADT7-Y2H-K54 (273SGB) cDNA. Screening was performed on selective medium (SD/-Trp-Leu-His-Ade) containing 5 mM 3-aminotriazole (3-AT), which tests the reporter gene ADE2, HIS3, and LacZ activated by positive PPP2R3A-target protein interaction. In order to reduce false positives, positive clones with a higher repetition

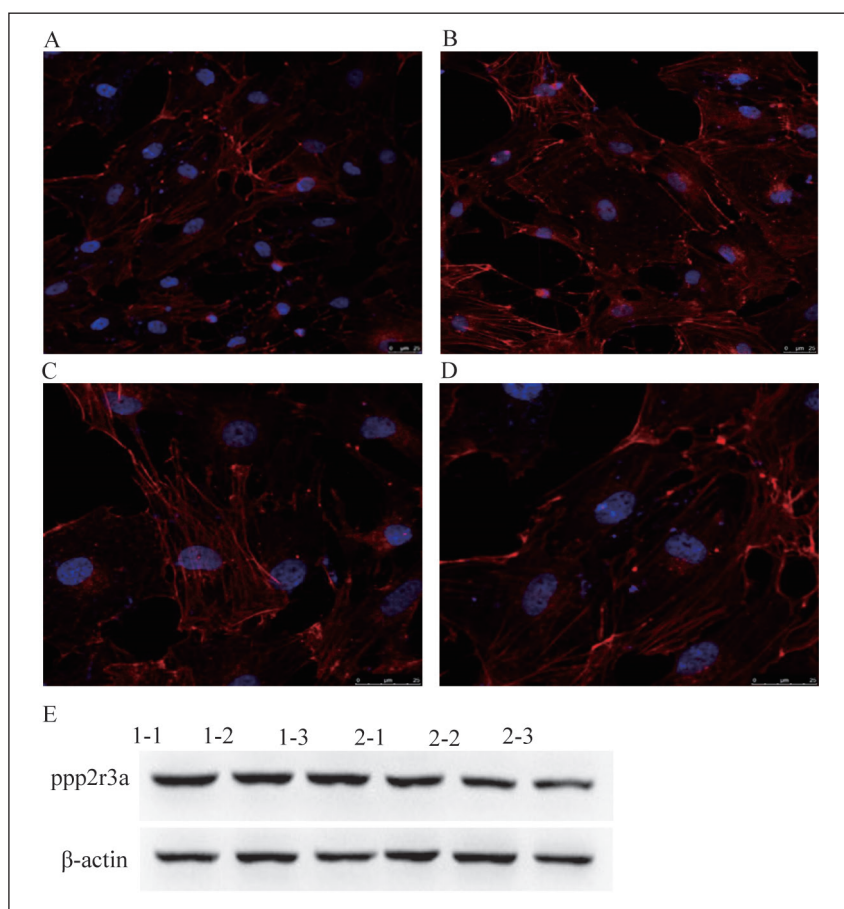


**Figure 1.** Immunofluorescence analysis for primary myocardial cell of neonatal rats *in vitro* and PPP2R3A protein levels in rat myocardial cells were detected by western blotting. **A-B**, immunofluorescence results of cultured primary myocardial cells (400 $\times$ ); **C-D**, immunofluorescence results of cultured primary myocardial cells (800 $\times$ ). **E**, 1-1, 1-2, 1-3, denoted H9c2 cells; 2-1, 2-2, 2-3, denoted primary cardiomyocytes. In all experiments,  $\beta$ -actin was utilized as a loading control.  $n=3$  for all experiments.

rate were reverted to verification. The positive candidates were isolated and sequenced, and homology searches against database sequences were performed using the BLAST algorithm on NCBI (National Center for Biotechnology Information).

### Statistical Analysis

All data are presented as mean  $\pm$  standard deviation. Statistical analysis was performed by one-way analysis of variance test. A  $p$ -value of  $<0.05$  was considered to be statistically significant.

## Results

### PPP2R3A Protein Content Determination

In order to show the cells in culture were primary cardiomyocytes, the  $\alpha$ -actin were labeled and imaged using fluorescence microscopy (Figure 1). There were numerous  $\alpha$ -actin positive cells, indicating cardiomyocytes were successfully isolated. Following the isolation of the neonatal rat cardiomyocytes, ppp2r3a were screened in the cardiomyocytes and H9c2 cell by Western blot-

ting. The results indicated that the ppp2r3a had the higher expression level. Together, the experiment offers the foundation to carry on function research of ppp2r3a for follow-up.

### Determination of ppp2r3a-Silencing Efficiency

To observe the silencing effect on Cardiomyocyte function *in vitro*, the viruses carrying ppp2r3a-silencing genes were transfected into rat primary cardiomyocytes cells and H9c2 cells. The silencing efficiency was assessed by reverse transcription PCR (Figure 2). The mRNA expression levels of ppp2r3a were decreased in the shRNA-transfected groups compared with the NC-shRNA groups, but shRNA#2-ppp2r3a was significantly decreased. Subsequently, the shRNA#2-ppp2r3a lentivirus particle was applied to carry out transient transfection in the above two cells, and the markedly decreased expression of ppp2r3a protein were observed in shRNA#2-ppp2r3a cells as compared to shRNA-control cells. This observation suggested that rat primary cardiomyocytes cells and H9c2 cells silencing ppp2r3a was successfully established.

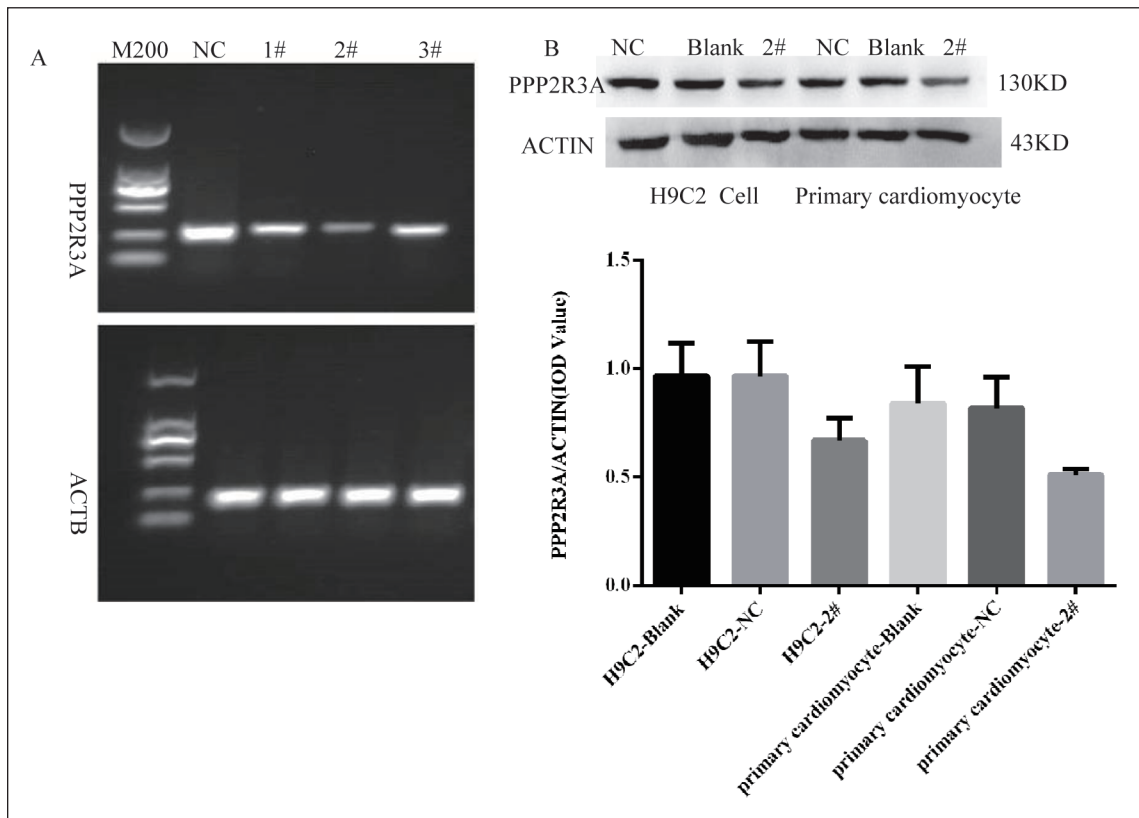


**Figure 2.** Ppp2r3a-silencing efficiency as well as protein levels detected. **A**, Ppp2r3a-silencing efficiency detected by reverse transcription PCR. NC, negative control;  $\beta$ -actin was utilized as a loading control. The shRNA#2-ppp2r3a lentivirus particles showed optimal interference efficiency. **B**, Ppp2r3a protein levels in H9c2 cells and primary cardiomyocytes were detected by western blotting.  $\beta$ -actin was utilized as a loading control.

### Effect of ppp2r3a Silencing on Cardiomyocytes Proliferation

To evaluate the effects of *ppp2r3a* silencing on the proliferation of rat primary cardiomyocytes cells and H9c2 cells, we employed Cell Counting Kit-8 (CCK-8) methods to study cell proliferation. According to the results, there was significant difference in  $OD_{450}$  value both in shRNA#2-*ppp2r3a* group and shRNA-control at 24h ( $p < 0.05$ ) (Table I), indicating that *ppp2r3a* silencing can slower growth rate and inhibit myocardial cell proliferation.

### Ppp2r3a Silencing Reduced the Proportion of Cardiomyocytes in S Phase

We observed that silencing *ppp2r3a* inhibited rat primary cardiomyocytes cells and H9c2 cells proliferation. Next, the distribution of different phases of cell cycling was determined. Our results showed that the percentage of S phase cells was significantly lower in shRNA#2-*ppp2r3a* group

(26.35% in H9c2 cells; 23.23% in rat primary cardiomyocytes cells) than that in shRNA-control (30.43% in H9c2 cells; 26.89% in rat primary cardiomyocytes cells) ( $p < 0.05$ ) (Figure 3, Table II). These data demonstrated that silencing *ppp2r3a* arrested the cell cycle in the S phase to inhibit the growth of cardiomyocytes cells.

### Ppp2r3a Silencing Accelerated Cardiomyocytes Apoptosis

Apoptosis is one of the major cell death pathways. Next, we tested whether *ppp2r3a* silencing affected the apoptosis of cardiomyocyte. As shown in Figure 4, the percentage of early apoptotic cells was mildly increased in *ppp2r3a* silencing group compared with in the control group.

### Construction of cDNA Library

In order to determine the interaction partners of the PPP2R3A protein, it is necessary to obtain a high-quality human primary cardiomyocyte cDNA library. To investigate the quality of

**Table I.** Cell proliferation results in H9c2 cells and primary cardiomyocytes by CCK-8 assay.

Groups	OD Value				p-value	
	1	2	3	Mean		Abs
Blank	0.0427	0.0392	0.0369	0.0396		
H9c2	1.2991	1.3017	1.264	1.2883	1.2487	
	1.3039	1.2822	1.2739	1.2867	1.2471	
	1.2872	1.2487	1.2174	1.2511	1.2115	
H9c2-NC	1.2867	1.2543	1.2345	1.2585	1.2189	
	1.2771	1.2594	1.2421	1.2595	1.2199	
	1.2035	1.1884	1.1632	1.1850	1.1454	
H9c2-2#	1.1021	1.0619	1.0876	1.0839	1.0443	<0.05*
	1.0834	1.1508	1.0983	1.1108	1.0712	
	1.0677	1.1395	1.0821	1.0964	1.0568	
Primary cardiomyocytes	1.1995	1.1549	1.2272	1.1939	1.1543	
	1.2512	1.1928	1.2106	1.2182	1.1786	
	1.2129	1.2637	1.2341	1.2369	1.1973	
Primary cardiomyocytes-NC	1.1467	1.1711	1.1639	1.1606	1.1210	
	1.1835	1.1684	1.1932	1.1817	1.1421	
	1.1676	1.1186	1.1788	1.1550	1.1154	
Primary cardiomyocytes-2#	1.0748	0.9935	1.0167	1.0283	0.9887	<0.05*
	1.0878	1.0797	1.0423	1.0699	1.0303	
	1.0762	1.0341	1.0679	1.0594	1.0198	

\*:compare with NC group.

the full-length cDNA library, the lengths of the cDNA inserts were amplified by PCR using primers. It is showed that no nonspecific bands were identified, and the majority of the cDNA inserts were more than 1200 bp in size (Figure 5). The recombination rate of cDNA library was 100%. The final library titer was  $1.2 \times 10^7$  CFU/ml which was consistent with expected. The sequence data were searched in the NCBI GenBank using BLAST to identify similarities with sequences in the nucleic acid databases. These findings indicated that the library could be used for further research.

#### **Construction of Bait Vector and Characterization of its Self-Activation in Yeast Cells**

To construct the PPP2R3A gene cDNA clone into the bait vector of Y2H, the recombinant plasmid pGADT7-PPP2R3A cut by incision enzyme SfiI overnight and connected with the bait vector plasmid pGBKT7. It was verified that the positive plasmid was successfully transformed into yeast Y2H which generated a 2kb fragment using the primers of PPP2R3A-F and PPP2R3A-R. Testing bait for autoactivation, the results showed that the yeast transfected with plasmids of pGBKT7-PPP2R3A could not grow on SD-TLHA agar plate and does not autonomously activate the re-

porter gene ADE2, HIS3 and LacZ in AH109, in the absence of a prey protein. So, we can believe that our PPP2R3A bait cloning is not self-activation in yeast (Figure 6). This work provides the basis for further experiments.

#### **Screening of PPP2R3A Interaction Proteins**

We performed yeast two-hybrid screening of the human primary cardiomyocyte's cDNA library using PPP2R3A as bait to identify new-PPP2R3A binding partners. A total of 24 preys still showed positive interaction with the bait, which were confirmed by clones' growth on selective media SD-TLHA and high stringency to activate the reporter gene LacZ (Figure 7). We sequenced these plasmids extracted from 24 positive clones with a higher repetition rate and found that 19 genes were identified as candidate positive interactions through NCBI/BLAST search, and the corresponding proteins were expressed respectively (Table III). To reduce false positives, the yeast AH109 containing the plasmid baits pGBKT7-PPP2R3A was co-transfected with 24 positive clones. The results showed that 24 positive clones belonged to 19 different protein-coding genes and all of them could activate ADE2, HIS3 and LacZ expression, suggesting that these

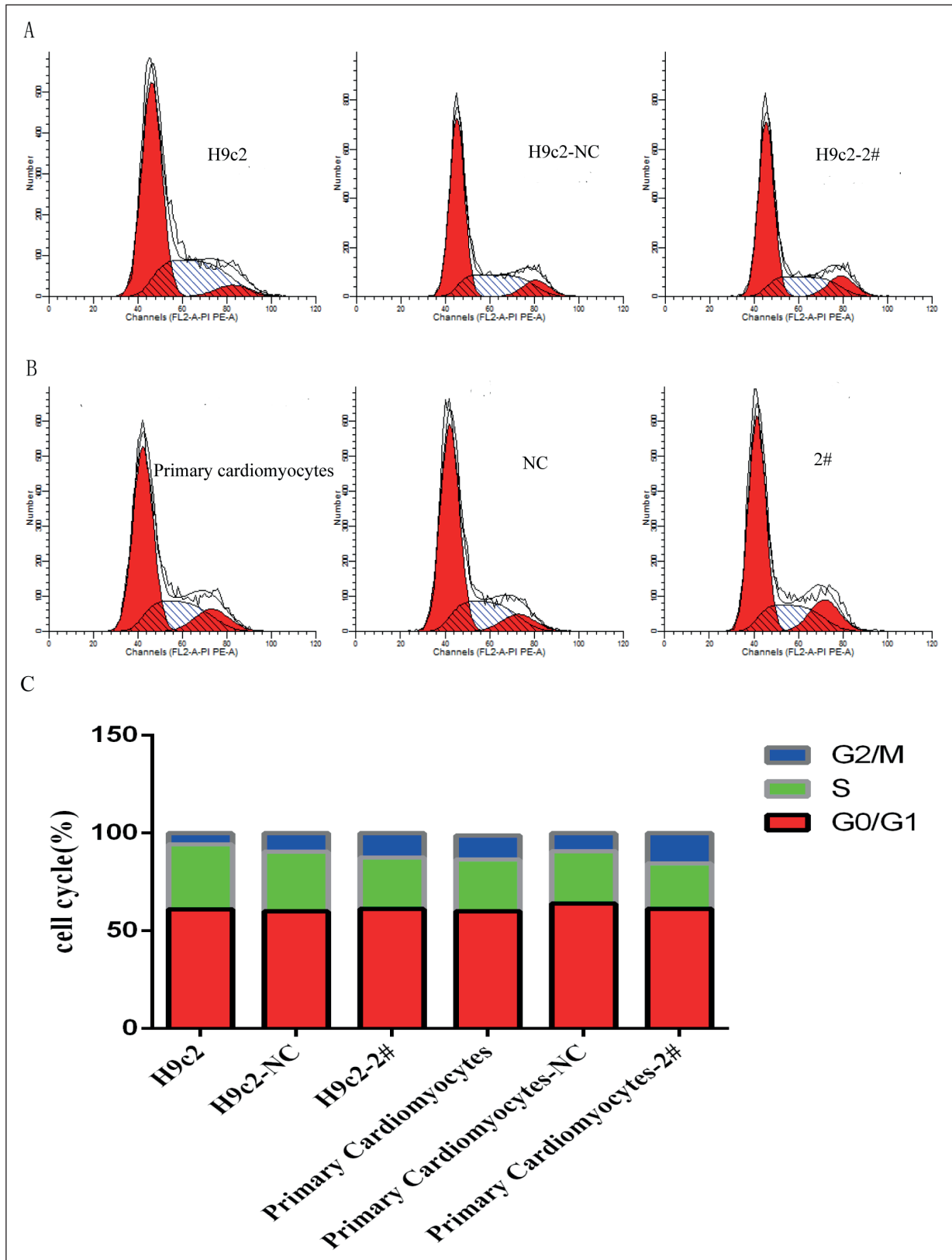


**Figure 3.** Ppp2r3a protein levels in H9c2 cells and primary cardiomyocytes were detected by western blotting.  $\beta$ -actin was utilized as a loading control. **A**, The original map; **B**, Cell cycle results in H9c2 cells and primary cardiomyocytes by flow cytometer. **C**, Statistic graphics of cell cycle results.

**Table II.** Cell cycle results in H9c2 cells and primary cardiomyocytes by flow cytometer.

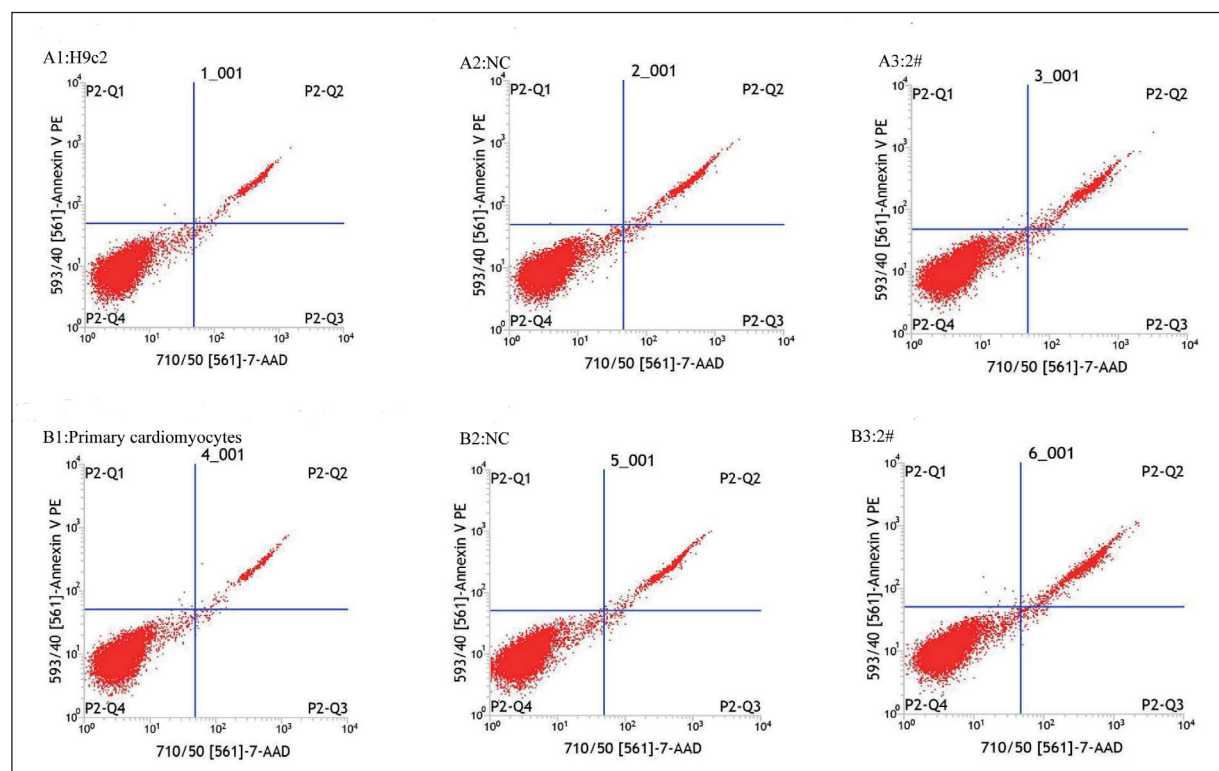
Groups	Mean			p-value
	G0/G1 (%)	S (%)	G2/M (%)	
H9c2	60.95	33.65	5.40	
H9c2-NC	59.91	31.00	9.10	
H9c2-2#	61.49	27.00	11.45	<0.05*
Primary cardiomyocytes	59.42	27.89	12.69	
Primary cardiomyocytes-NC	63.34	27.23	9.43	
Primary cardiomyocytes-2#	61.06	23.62	15.32	<0.05*

\*:compare with NC group.

proteins specifically interact with PPP2R3A (Figure 8). Among them, three proteins (COL1A2, GIPC1 and BCL6) presented the higher screening frequency, and COL1A2 was the highest, covering 12.5% of the 24 clones. Gene Ontology biological processes were constructed using Metascape. 19 genes were strongly mapped to 3 major modules. The majority of the pathways in the first module were associated with the signaling, implying that PPP2R3A-partner (like COL1A2, GIPC1 and BCL6) regulated myocardial function by a complex set of pathways.

## Discussion

The regulatory subunits of PP2A are coded by at least 17 distinct genes and at least 11 of them are expressed in cardiomyocytes. B56 $\alpha$  and B56 $\gamma$  are the most studied cardiac isoforms<sup>4</sup>, and relatively little is known about the role of PPP2R3A in the heart. The major findings of the present study were as follows: (1) primary cardiomyocytes of neonatal rats were established successfully; (2) *ppp2r3a* was highly expressed in the myocardial cells; (3) *ppp2r3a* silencing could inhibit myocar-

**Figure 4.** Cell apoptosis results in H9c2 cells and primary cardiomyocytes by flow cytometer.



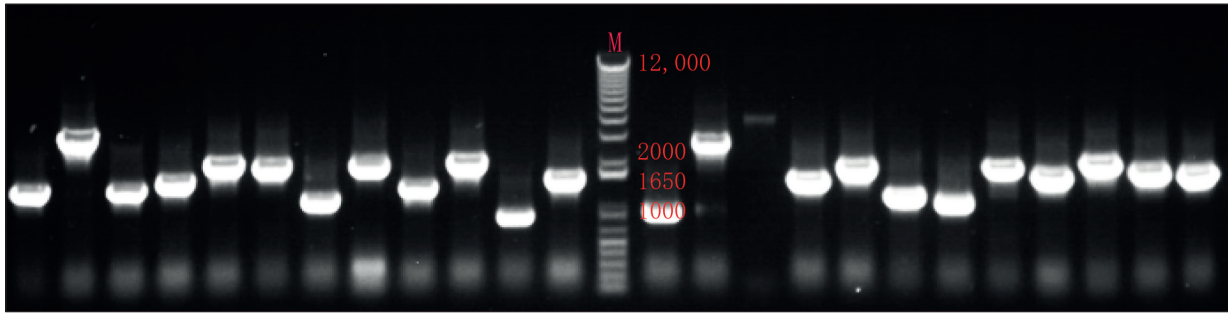


**Figure 5.** Quality of cDNA library. The PCR products of 23 clones showed that the bands of cDNA fragments ranged from 1.0 to 2.0kb in size.

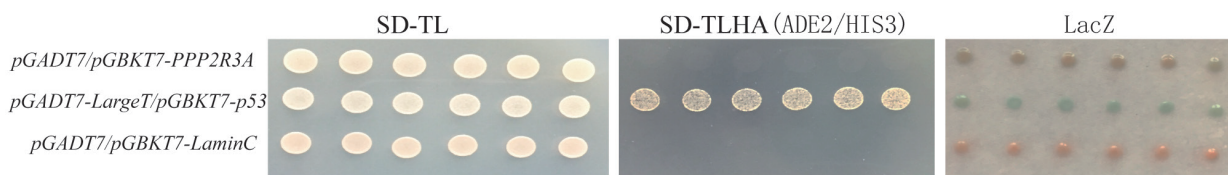


**Figure 6.** Confirmation of the interaction in the bait vector pGBKT7-PPP2R3A. The Y2H yeast cells that were co-transformed pGADT7 with and pGBKT7-PPP2R3A were plated on synthetically defined (SD) medium lacking leucine (Leu) and tryptophan (Trp) (SD/-Leu/-Trp), and histidine (His) as well as adenine (SD/-Leu/-Trp/-His/-adenine), and cultivated for 4 days at 30°C. The transformants cannot grow normally on SD-TL and SD-TLHA defective plates and did not turn blue in the  $\beta$ -galactosidase assay, indicating that pGBKT7-PPP2R3A does not autonomously activate the reporter genes in yeast cells without a prey protein. Co-transformation with pGADT7 and pGBKT7-p53, pGBKT7-LaminC was used as a positive control and negative control respectively.

dial cell proliferation by arrested the cell cycle in the S phase; (4) *ppp2r3a* silencing could mildly increase early apoptosis of cardiomyocytes; (5) 19 proteins putatively interacted with PPP2R3A and the majority of the pathways were associated with the signaling. These results suggested that *ppp2r3a* knockdown can damage cardiac

function, implying that *ppp2r3a* might display important roles in normal cardiac function and PPP2R3A in the regulation of cardiac events *via* its interaction partners.

Cell culture of cardiomyocytes is a critical tool in modern cardiac research and has been widely employed as experimental model to study

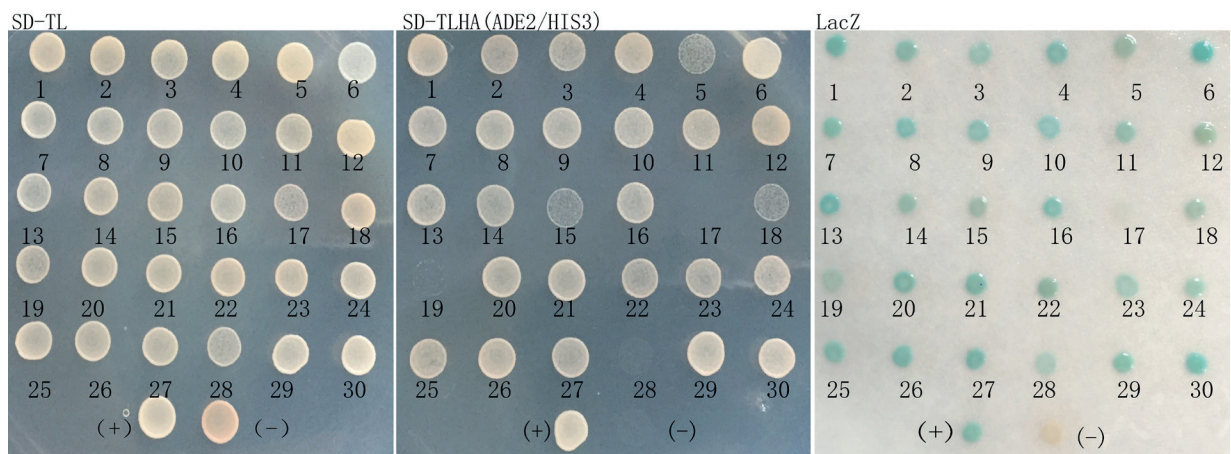


**Figure 7.** Confirmation of the interaction between the human primary cardiomyocytes' cDNA library and pGBKT7-PPP2R3A by Y2H assays. The 30 colonies were plated on SD/-Leu/-Trp, and SD/-Leu/-Trp/-His/-adenine plates and cultivated for 4 days at 30°C. 24 positive interaction was indicated by the growth of SD/-Leu/-Trp/-His/-adenine plates and the presence of blue colonies on filter paper. The positive control colony were light blue and negative control was not displayed in blue.

**Table III.** The BLAST results of positive interacting proteins from the pGBKT7-PPP2R3A bait.

No.	GenBank accession No.	Protein Name	Appearance
1	XM_011543989.2	Homo sapiens RNA binding motif protein 10 (RBM10)	1
2	NM_202470.2	Homo sapiens GIPC PDZ domain containing family member 1 (GIPC1)	2, 3
3	XM_017023746.1	Homo sapiens axin 1 (AXIN1)	6
4	NM_000089.3	Homo sapiens collagen type I alpha 2 (COL1A2)	7, 8, 10
5	NM_006806.4	Homo sapiens BTG anti-proliferation factor 3 (BTG3)	9
6	NM_002775.4	Homo sapiens HtrA serine peptidase 1 (HTRA1)	12
7	XM_017028666.1	Homo sapiens EWS RNA binding protein 1 (EWSR1)	13
8	XM_016999458.1	Homo sapiens NUT family member 2B (NUTM2B)	4
9	XM_011539975.2	Homo sapiens chromosome 10 open reading frame 2 (C10orf2)	16
10	XM_005247694.3	Homo sapiens B-cell CLL/lymphoma 6 (BCL6)	11, 20
11	XM_017025144.1	Homo sapiens myosin XVb (MYO15B)	21
12	NM_001317735.1	Homo sapiens pre-B-cell leukemia homeobox interacting protein 1 (PBXIP1)	22
13	BC066956.1	Homo sapiens vimentin	23
14	NM_182709.2	Homo sapiens lysine acetyltransferase 5 (KAT5)	24
15	NM_199512.2	Homo sapiens coiled-coil domain containing 80 (CCDC80)	25
16	XM_004062568.2	Gorilla gorilla gorilla regulator of G-protein signaling 19 (RGS19)	26
17	KU178806.1	Homo sapiens zinc finger CCCH-type with G patch domain isoform 1 (ZGPAT)	14, 27
18	XM_017013308.1	Homo sapiens KIAA1429 (KIAA1429)	29
19	XM_011527860.2	Homo sapiens histocompatibility (minor) HA-1 (HMHA1)	30

cardiac pathophysiology. Previous studies have shown that cardiomyocytes derived from embryonic stem cells (ESCs) or induced pluripotent stem cells (iPSCs) have been shown to exhibit differences in electrophysiology from primary cardiomyocytes and the reprogramming and/or differentiation process can be time consuming and costly<sup>8</sup>. The primary culture of neonatal mice cardiomyocyte model enables to study and understand the morphological, biochemical, and electrophysiological characteristics of the heart<sup>9</sup>. Therefore, we utilized neonatal rat cardiomyocytes (NRCM) due to its isolation and culture is easier, efficient, and it has many features. One challenge to NRCM isolation and culture is the rapid proliferation of fibroblasts. In our study, large amounts of NRCM were isolated successfully from fibroblasts through the exchange of the cell medium and using uncoated flasks. This was coincident with the numerous  $\alpha$ -actin positive cells using fluorescence microscopy.

Next, we observed that *ppp2r3a* is expressed in the myocardial cells with a relatively higher level. The results were consistent with earlier study showing that PR130, the largest transcript of PPP2R3A, was detected in almost all tissues, but

with highest levels in heart and muscle, whereas PR72, another transcript of PPP2R3A, was expressed exclusively in heart and skeletal muscle<sup>10</sup>. In addition, we also observed that silencing notably interrupted the cardiac function. A recent study<sup>7</sup> showed that PR130-knockout exhibited cardiac looping defects, decreased cardiac function and fractional area, and increased apoptosis *via* reduced PP2A activity in the Zebrafish. Similarly, pr72 knockout zebrafish also exhibited cardiac developmental defects, including enlarged ventricular chambers, reduced cardiomyocytes and decreased cardiac function<sup>11</sup>.

A further study<sup>12</sup> revealed that PR72 mediated  $\text{Ca}^{2+}$ -dependent dephosphorylation at Thr-75 of DARPP-32 to affect the PP2A activity. Besides, dephosphorylation of RyR2 was controlled by PP2A *via* binding with PR130<sup>13</sup>. Taken together, PPP2R3A is the regulatory subunit of PP2A, where it appears to mediate the interaction between the PP2A heterodimer and its targeting substrates in cardiomyocytes. Thereby, we speculated that PPP2R3A silencing is likely to interrupt the cardiac performance *via* altered PP2A activity to defected dephosphorylation on cardiac important proteins.



**Figure 8.** Candidate positive clone's re-hybrid. with pGBKT7-PPP2R3A. 24 positive clones were co-transfected with bait plasmid pGBKT7-PPP2R3A, then were plated on SD/-Leu/-Trp, and SD/-Leu/-Trp/-His/-adenine plates to cultivate for 5 days at 30°C. All the 24 positive clones could activate His and Ade reporter genes on the SD/-Leu/-Trp/-His/-adenine plates and can turn blue in the  $\beta$ -galactosidase assay.

In fact, PP2A plays an important role in development, cell proliferation and death, cell mobility, cytoskeleton dynamics, the control of the cell cycle, and the regulation of numerous signaling pathways<sup>14</sup>. In the heart, PP2A is mainly responsible for dephosphorylating L-type  $\text{Ca}^{2+}$  channel<sup>15-17</sup>, the ryanodine receptor (RyR2)<sup>18</sup>, cTnI etc<sup>19-20</sup>. That is, PP2A is critical molecules in cellular excitability and myocardial contractility *via* interacting with multiple components. Our study reflected that *ppp2r3a* silencing could inhibit myocardial cell proliferation and mildly increase early apoptosis of cardiomyocytes.

The phosphorylation and dephosphorylation of proteins mediated by PP2A plays a pivotal role in the control of a variety of cellular processes. However, the relationship between the downstream targets of PP2A and the proliferation and differentiation of cardiomyocytes remains to be further explored. In this paper, we identified 19 proteins that putatively interacted with PPP2R3A. Among them, three proteins (COL1A2, GIPC1 and BCL6) presented the higher screening frequency with 24 clones. In particular, COL1A2 was the highest, covering 12.5% of the 24 clones. It well known that the collagen synthesized by cardiac fibroblasts is required to maintain the integrity and biomechanical properties of the heart, of which type I collagen (COL1) represents ~80% of the total newly synthesized collagen<sup>21</sup>. COL1 is composed of two chains,  $\alpha 1$  (COL1A1) and  $\alpha 2$ . Functional COL1 consists of two  $\alpha 1$  chains and one  $\alpha 2$  chain tightly coiled around each other in a triple helix and become covalently cross-linked forming long fibrils, which provide a structural support for the attachment of cells and other extracellular matrix components<sup>22</sup>. Previous studies have identified its roles in common heart disor-

ders. For example, COL1A2 was highly expressed after myocardial infarction (MI) and hypertrophic cardiomyopathy<sup>23,24</sup>. COL1 also plays important roles during cardiac remodeling if which fails to be inactivated, resulting in fibrosis and cardiac dysfunction<sup>25</sup>. Recently, the research revealed that COL1 can reduce PP2A activity to enhance the differentiation and proliferation of myofibroblasts in MI<sup>26</sup>. Together, we proposed that interaction of COL1A2 and PPP2R3A might alter the activity of PPP2R3A to permit aberrant differentiation and proliferation on cardiomyocytes.

The GIPC1 gene (also known as C19orf3) located at human chromosome 19p13.12 and consist of GIPC homology 1 (GH1) domain, PDZ domain and GH2 domain<sup>27</sup>. Physiological roles of GIPC1 have been well characterized. GIPC1 is a cytoplasmic protein that acts as an adaptor protein, linking receptor interactions to intracellular signaling pathways to regulate a variety of cellular processes, including cell cycle regulation<sup>28</sup>. Growing evidence shows that proteins usually do not act as a single substance but rather as team participant in a dynamic network, this is possible knock-down of *ppp2r3a* has effect on cell cycle of cardiomyocytes through the interaction PPP2R3A of and GIPC1.

B-cell lymphoma 6 (BCL6) on chromosome 3, band q27 is initially discovered as an oncogene in B-cell lymphomas. BCL6 protein is an evolutionarily conserved zinc finger transcription factor with an N-terminal POZ/BTB domain. This protein can form complexes with corepressors *via* protein-protein interactions (PPIs) to inhibit transcription and functions as a sequence-specific transcriptional repressor<sup>29</sup>. Many studies<sup>30-32</sup> have been focused on the effect of Bcl6 on cancer development, progress and metastasis. Recently, Gu et al<sup>33</sup> observed that Bcl6 knockdown aggravated hypoxia injury in

cardiomyocytes, and Jian et al<sup>34</sup> Bcl6 explored the functional role of Bcl6 in cardiac fibroblast activation and function. Given that all these data suggest the candidate protein is considered to be associated with the cardiovascular diseases and are potential disease-related proteins.

## Conclusions

In summary, we provide new evidence that PPP2R3A plays an important role in maintaining normal myocardial function. Several important interacting proteins (like COL1A2, GIPC1 and BCL6) may participate in this series of complex signal networks. Hence, it is expected to be a potential therapeutic target for the disease. However, its interaction with that kind of specific protein, how it works, and which way it does need to further research.

## Acknowledgement

This work was supported by grants from the National Natural Science Foundation of China (Grant No: 81460064), General Project of Science and Technology Department of Yunnan Province-Kunming Medical University Union Fund (Grant No: 2014FB034) and Yunnan health training project of high-level talents (Grant No: H-2018075).

## Conflicts of Interest

The authors declare no conflict of interest.

## References

- Heijman J, Dewenter M, El-Armouche A, Dobrev D. Function and regulation of serine/threonine phosphatases in the healthy and diseased heart. *J Mol Cell Cardiol* 2013; 64: 90-98.
- DeGrande ST, Little SC, Nixon DJ, Wright P, Snyder J, Dun W, Murphy N, Kilic A, Higgins R, Binkley PF, Boyden PA, Carnes CA, Anderson ME, Hund TJ, Mohler PJ. Molecular mechanisms underlying cardiac protein phosphatase 2A regulation in heart. *J Biol Chem* 2013; 288: 1032-1046.
- Lubbers ER, Mohler PJ. Roles and regulation of protein phosphatase 2A (PP2A) in the heart. *J Mol Cell Cardiol* 2016; 101: 127-133.
- Varadkar P, Despres D, Kraman M, Lozier J, Phadke A, Nagaraju K, Mccright B. The protein phosphatase 2A B56γ regulatory subunit is required for heart development. *Dev Dyn* 2014; 243: 778-790.
- Hendrix P, Mayer-Jackel RE, Cron P, Goris J, Hofsteenge J, Merlevede W, Hemmings BA. Structure and expression of a 72-kDa regulatory subunit of protein phosphatase 2A. Evidence for different size forms produced by alternative splicing. *J Biol Chem* 1993; 268: 15267-15276.
- Little SC, Curran J, Makara MA, Kline CF, Ho HT, Xu Z, Wu X, Polina I, Musa H, Meadows AM, Carnes CA, Biesiadecki BJ, Davis JP, Weisleder N, Györke S, Wehrens XH, Hund TJ, Mohler PJ. Protein phosphatase 2A regulatory subunit B56α limits phosphatase activity in the heart. *Sci Signal* 2015; 8: ra72.
- Yang J, Li Z, Gan X, Zhai G, Gao J, Xiong C, Qiu X, Wang X, Yin Z, Zheng F. Deletion of Pr130 Interrupts Cardiac Development in Zebrafish. *Int J Mol Sci* 2016; 17: 1746.
- Vandergriff AC, Hensley MT, Cheng K. Isolation and cryopreservation of neonatal rat cardiomyocytes. *J Vis Exp* 2015; 98: 52726.
- Sreejit P, Kumar S, Verma RS. An improved protocol for primary culture of cardiomyocyte from neonatal mice. *In Vitro Cell Dev Biol Anim* 2008; 44: 45-50.
- Zwaenepoel K, Louis JV, Goris J, Janssens V.X. Diversity in genomic organisation, developmental regulation and distribution of the murine PR72/B<sup>γ</sup> subunits of protein phosphatase 2A. *BMC Genomics* 2008; 9: 393.
- Guibo Song, Mingjun Han, Zuhua Li, Xuedong Gan, Xiaowen Chen, Jie Yang, Sufang Dong, Ming Yan, Jun Wan, Yanggan Wang, Zhuliang Huang, Zhan Yin, Fang Zheng. Deletion of Pr72 causes cardiac developmental defects in Zebrafish. *PLoS One* 2018; 3: e0206883.
- Ahn JH, Sung JY, McAvoy T, Nishi A, Janssens V, Goris J, Greengard P, Nairn AC. The B<sup>γ</sup>/PR72 subunit mediates Ca<sup>2+</sup>-dependent dephosphorylation of DARPP-32 by protein phosphatase 2A. *Proc Natl Acad Sci* 2007; 104: 9876-9881.
- Belevych AE, Sansom SE, Terentyeva R, Ho HT, Nishijima Y, Martin MM, Jindal HK, Rochira JA, Kunitomo Y, Abdellatif M, Carnes CA, Elton TS, Györke S, Terentyev D. MicroRNA-1 and -133 increase arrhythmogenesis in heart failure by dissociating phosphatase activity from RyR2 complex. *PLoS One* 2011; 6: e28324.
- Shi Y. Serine/threonine phosphatases: mechanism through structure. *Cell* 2009; 139: 468-484.
- Xu H, Ginsburg KS, Hall DD, Zimmermann M, Stein IS, Zhang M, Tandan S, Hill JA, Horne MC, Bers D, Hell JW. Targeting of protein phosphatases PP2A and PP2B to the C-terminus of the L-type calcium channel Cav1.2. *Biochemistry* 2010; 49: 10298-10307.
- Hall DD, Feekes JA, Arachchige Don AS, Shi M, Hamid J, Chen L, Strack S, Zamponi GW, Horne MC, Hell JW. Binding of protein phosphatase 2A to the L-type calcium channel Cav1.2 next to Ser1928, its main PKA site, is critical for Ser1928 dephosphorylation. *Biochemistry* 2006; 45: 3448-3459.
- Shi J, Gu P, Zhu Z, Liu J, Chen Z, Sun X, Chen W, Gao X, Zhang Z. Protein phosphatase 2A effectively modulates basal L-type Ca<sup>2+</sup> current by dephosphorylating Ca(v)1.2 at serine 1866 in mouse cardiac myocytes. *Biochem Biophys Res Commun* 2012; 418: 792-798.
- Terentyev D, Belevych AE, Terentyeva R, Martin MM, Malana GE, Kuhn DE, Abdellatif M, Feldman DS, Elton TS, Györke S. miR-1 overexpression enhances Ca<sup>2+</sup> release and promotes cardi-

- ac arrhythmogenesis by targeting PP2A regulatory subunit B56 $\alpha$  and causing CaMKII-dependent hyperphosphorylation of RyR2. *Circ Res* 2009; 104: 514-521.
- 19) Solaro RJ, Kobayashi T. Protein phosphorylation and signal transduction in cardiac thin filaments. *J Biol Chem* 2011; 286: 9935-9940.
  - 20) Wijinker PJ, Boknik P, Gergs U, Müller FU, Neumann J, dos Remedios C, Schmitz W, Sindermann JR, M Stienen GJ, van der Velden J, Kirchhefer U. Protein phosphatase 2A affects myofilament contractility in non-failing but not in failing human myocardium. *J Muscle Res Cell Motil* 2011; 32: 221-233.
  - 21) Yin Z, Guo Y, Zhang J, Zhang Q, Li L, Wang S, Wang C, He Y, Zhu S, Li C, Zhang S, Zha L, Cai J, Luo B, Gao Y. Association between an indel polymorphism in the 3'UTR of COL1A2 and the risk of sudden cardiac death in Chinese populations. *Leg Med (Tokyo)* 2017; 28: 22-26.
  - 22) Papaioannou I, Xu S, Denton CP, Abraham DJ, Ponticos M. STAT3 controls COL1A2 enhancer activation cooperatively with JunB, regulates type I collagen synthesis posttranscriptionally, and is essential for lung myofibroblast differentiation. *Mol Biol Cell* 2018; 29: 84-95.
  - 23) Small EM, Thatcher JE, Sutherland LB, Kinoshita H, Gerard RD, Richardson JA, Dimaio JM, Sadek H, Kuwahara K, Olson EN. Myocardin-related transcription factor-A controls myofibroblast activation and fibrosis in response to myocardial infarction. *Circ Res J* 2010; 107: 294-304.
  - 24) Marian AJ, Senthil V, Chen SN, Lombardi R. Antifibrotic Effects of Antioxidant N-Acetylcysteine in a Mouse Model of Human Hypertrophic Cardiomyopathy Mutation. *J Am Coll Cardiol* 2006; 47: 827-834.
  - 25) Jugdutt BI. Remodeling of the myocardium and potential targets in the collagen degradation and synthesis pathways. *Curr Drug Targets Cardiovasc Haematol Disord* 2003; 3: 1-30.
  - 26) Hong J, Chu M, Qian L, Wang J, Guo Y, Xu D. Proliferation and Proliferation of Myofibroblasts by Lowering  $\alpha$ 2 $\beta$ 1 Integrin Expression in Cardiac Fibrosis. *Biomed Res Int* 2017; 1790808.
  - 27) Kato M. Functional proteomics, human genetics and cancer biology of GIPC family members. *Exp Mol Med* 2013; 45: e26.
  - 28) Bao L, Guo T, Wang J, Zhang K, Bao M. Prognostic genes of triple-negative breast cancer identified by weighted gene co-expression network analysis. *Oncol Lett* 2020; 19: 127-138.
  - 29) Chen D, Zang YH, Qiu Y, Zhang F, Chen AD, Wang JJ, Chen Q, Li YH, Kang YM, Zhu GQ. BCL6 Attenuates Proliferation and Oxidative Stress of Vascular Smooth Muscle Cells in Hypertension. *Oxid Med Cell Longev* 2019; 5018410.
  - 30) Mariano G Cardenas, Erin Oswald, Wenbo Yu, Fengtian Xue, Alexander D MacKerell Jr, Ari M Melnick. The Expanding Role of the BCL6 Oncoprotein as a Cancer Therapeutic Target. *Clin Cancer Res* 2017; 23: 885-893.
  - 31) Lin Ang, Li Zheng, Jin Wang, Jin Huang, Hong-Guang Hu, Qiang Zou, Yang Zhao, Qiang-Ming Liu, Min Zhao, Zheng-Sheng Wu. Expression of and correlation between BCL6 and ZEB family members in patients with breast cancer. *Exp Ther Med* 2017; 14: 3985-3992.
  - 32) Liancheng Zhu, Huilin Feng, Shan Jin, Mingzi Tan, Song Gao, Huiyu Zhuang, Zhenhua Hu, Huimin Wang, Zuofei Song, Bei Lin. High expressions of BCL6 and Lewis y antigen are correlated with high tumor burden and poor prognosis in epithelial ovarian cancer. *Tumour Biol* 2017; 39: 1010428317711655.
  - 33) Gu Y, Luo M, Li Y, Su Z, Wang Y, Chen X, Zhang S, Sun W, Kong X. Bcl6 knockdown aggravates hypoxia injury in cardiomyocytes via the P38 pathway. *Cell Biol Int* 2019; 43: 108-116.
  - 34) Ni J, Wu QQ, Liao HH, Fan D, Tang QZ. Bcl6 Suppresses Cardiac Fibroblast Activation and Function via Directly Binding to Smad4. *Curr Med Sci* 2019; 39: 534-540.